PHYSICAL REVIEW B **82**, 064511 (2010)

Unconventional superconducting phase in the weakly correlated noncentrosymmetric Mo_3Al_2C compound

E. Bauer,[1] G. Rogl,[2] Xing-Qiu Chen,[3] R. T. Khan,[1] H. Michor,[1] G. Hilscher,[1] E. Royanian,[1] K. Kumagai,[4] D. Z. Li,[3] Y. Y. Li,[3] R. Podloucky,[2] and P. Rogl[2]

[1]*Institute of Solid State Physics, Vienna University of Technology, A-1040 Wien, Austria*

[2]*Institute of Physical Chemistry, University of Vienna, A-1090 Wien, Austria*

[3]*Shenyang National Laboratory for Materials Science, Institute of Metal Research, Chinese Academy of Sciences, Shenyang, China*

[4]*Division of Physics, Graduate School of Science, Hokkaido University, Sapporo 060-0810, Japan*

(Received 29 March 2010; revised manuscript received 30 July 2010; published 17 August 2010)

Electrical resistivity, specific-heat, and NMR measurements classify noncentrosymmetric Mo_3Al_2C (β-Mn type, space group $P4_132$) as a strong-coupled superconductor with $T_c=9$ K deviating notably from BCS-type behavior. The absence of a Hebbel-Slichter peak, a power-law behavior of the spin-lattice relaxation rate (from ^{27}Al NMR), an electronic specific heat strongly deviating from BCS model and a pressure enhanced T_c suggest unconventional superconductivity with possibly a nodal structure of the superconducting gap. Relativistic density-functional theory calculations reveal a splitting of degenerate electronic bands due to the asymmetric spin-orbit coupling, favoring a mix of spin-singlet and spin-triplet components in the superconducting condensate, in absence of strong correlations among electrons.

DOI: 10.1103/PhysRevB.82.064511 PACS number(s): 74.25.Bt, 72.15.Eb, 74.25.N−, 74.70.Ad

I. INTRODUCTION

Carbides based on Mo comprise a large body of refractory compounds, where carbon atoms (in trigonal prismatic or octahedral Mo_6C subunits) occupy a fraction of the interstitial sites either in an ordered or in a random manner. Among Mo-based carbides for which superconductivity (SC) was reported (αMoC at $T_c=9.95$ K, ηMoC at 7.57 K, Mo_2BC at 6.33 K, and Mo_3Al_2C at 9.05 K) the crystal structure of Mo_3Al_2C is outstanding since the respective β-Mn type does not possess a center of inversion.[1] The missing inversion symmetry might initiate a mixture of spin-singlet and spin-triplet pairs in the SC condensate[2] as was recently proposed to explain SC in $CePt_3Si$,[3] Ulr,[4] $CeRhSi_3$,[5] and $CeIrSi_3$.[6] Noncentrosymmetry (NCS) of the crystal structure introduces an electrical field gradient and, thereby, creates a Rashba-type antisymmetric spin-orbit coupling.[2]

The Ce- and U-based SCs indicated above are characterized by heavy-fermion behavior at low temperatures provoked by Kondo interaction. NCS in such systems can lead to new anomalous spin fluctuations, stabilizing triplet pairing, in addition to the singlet part.[7] On the other hand, a variety of SCs has been identified, which lacks strong electron correlations as well as a center of inversion. For a recent listing of these systems see Ref. 8. Except Li_2Pt_3B,[9] all yet studied NCS SCs without strong correlations among electrons are typical *s*-wave fully gapped BCS SC either weakly or strongly coupled.

In order to shed light onto the primary mechanism activating unconventional SC, we are searching for systems where SC occurs in absence of inversion symmetry, and also in absence of strong electron correlations. Revisiting Mo_3Al_2C (β-Mn structure), we aim to extend research done in the 1960s,[10] providing insight into microscopic features and the electronic structure.

II. EXPERIMENTAL

For the preparation of Mo_3Al_2C an elemental powder mixture (purity >99.9 mass%, about 5 g) was cold compacted, reacted in a high-vacuum furnace for 24 h at 1500 °C with one intermediate grinding and compacting step. Afterwards the material was ball milled and hot pressed at 1250 °C at 56 MPa. Refinement of the crystal structures was performed with the program FULLPROF.[11] Measurements of magnetic and transport properties were carried out with standard techniques.[12,13] Specific-heat measurements in the temperature range 2.1–160 K and magnetic fields up to 11 T were carried out on a 1.735 g sample employing an adiabatic step-heating technique. The sample holder consists of a thin sapphire disk ($m\sim0.2$ g) with a strain gauge heater and a CERNOX temperature sensor. The field calibration of the latter has been performed against two GaAlAs resistivity thermometers and a capacitive $SrTiO_3$ sensor. Additional zero-field heat-capacity measurements down to 375 mK were carried out with a ^{3}He Quantum Design PPMS calorimeter with a careful addenda calibration using synthetic α-Al_2O_3 (NIST reference material no. 720). The density-functional theory (DFT) calculations were performed with the Vienna *ab initio* simulation package (VASP).[14] For details see our recent paper on NCS $BaPtSi_3$.[8]

III. RESULTS AND DISCUSSION

X-ray Rietveld refinement confirmed a cubic, noncentrosymmetric structure (space group $P4_132$), isotypic to the β-Mn type; see Fig. 1). Measurements of the temperature-dependent electrical resistivity ρ of Mo_3Al_2C clearly evidences metallic behavior and indicate a SC phase transition at $T_c=9$ K (see Fig. 2), in agreement with the data reported by Johnston *et al.*[15] SC with almost 100% volume fraction is revealed from magnetic susceptibility measurements as well. Since the absolute resistivity values are large, the parallel resistance model (compare, e.g., Ref. 16) can be used to describe $\rho(T)$, where the ideal resistivity follows from the Bloch-Grüneisen model. A fit employing this model is shown in Fig. 2 as a solid line, revealing a Debye temperature θ_D

 ©2010 The American Physical Society

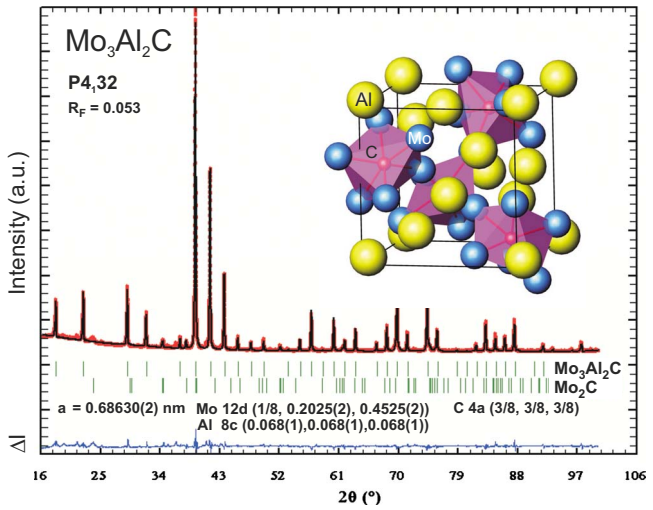

FIG. 1. (Color online) Rietveld refinement (Guinier-Huber image plate system, Cu $K_{\alpha 1}$) and crystallographic data of Mo_3Al_2C. The inset shows a three-dimensional view of the crystal structure. Traces of Mo_2C are indicated by vertical bars.

=286 K and a saturation value $\rho_{sat}=350\ \mu\Omega$ cm. An estimation of the electron-phonon interaction strength $\lambda_{e,ph}$ is possible in terms of the McMillan formula.[17] Applying this model, and taking the repulsive screened Coulomb part $\mu^* \approx 0.13$, yields $\lambda_{e,ph} \approx 0.8$; this characterizes Mo_3Al_2C as a SC well beyond the weak-coupling limit.

The pressure dependence of T_c of Mo_3Al_2C is displayed in the inset of Fig. 2. Obviously, $T_c(p)$ increases but tends to saturate for high pressures. An increase in T_c is rarely found in simple materials; rather, such a behavior frequently occurs in unconventional SCs like in high-temperature SCs, in various pyrochlores, in some Fe-pnictides, or heavy-fermion materials. Bogolyobov *et al.*[18] demonstrated that there are two principal parameters determining T_c: θ_D and the electronic density of states (DOS) at the Fermi energy, $N(E_F)$. Since the application of pressure hardly modifies $\rho(T,p)$ in the normal-state region (not shown here), $\theta_D(p)$ remains unchanged. Thus, a slight increase in $N(E_F)$ is concluded, enhancing T_c on pressurizing Mo_3Al_2C.

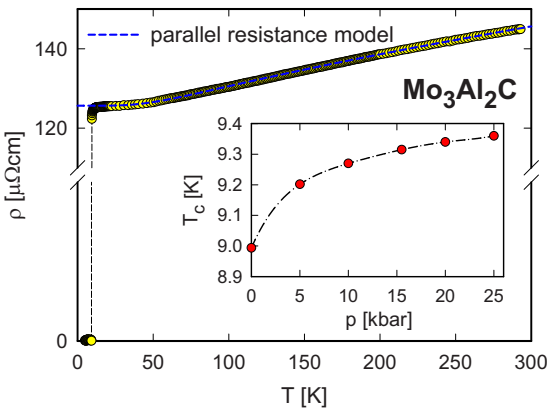

FIG. 2. (Color online) Temperature-dependent electrical resistivity ρ of Mo_3Al_2C. The dashed line is a least-squares fit according to the parallel resistance model. The inset shows the pressure dependence of T_c.

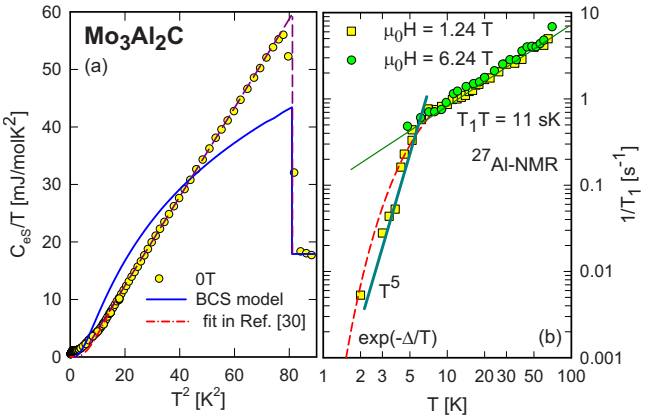

FIG. 3. (Color online) (a) Electronic specific-heat contribution $C_{eS}(T)$ of Mo_3Al_2C plotted as C_{eS}/T vs T^2. The dashed line is a guide for the eye and indicates an idealized superconducting phase transition together with a T^3 dependence of $C_p(T)$ for $T<T_c$. The solid line represents $C_p(T)$ of a spin-singlet fully gapped BCS superconductor according to Mühlschlegel (Ref. 19). The dashed-dotted line indicates an exponential temperature dependence suggested in Ref. 30. (b) Temperature-dependent $1/T_1$ ^{27}Al NMR relaxation rate deduced at $\mu_0 H=1.24$ and 6.95 T. The solid lines are guides for the eye. The dashed line represents an exponential temperature dependence.

Figure 3(a) shows the electronic temperature-dependent specific heat $C_{eS}(T)$ of Mo_3Al_2C taken at 0 T and plotted as C_{eS}/T vs T^2. For subtracting the phonon background, high-field measurements were extrapolated to $T\rightarrow 0$ using a Debye temperature $\theta_D=315$ K (see also below). Bulk SC is evidenced from a distinct anomaly at 9 K, rendering the onset of the SC phase transition. A closer inspection of the data gives evidence of various non-BCS-type features: (i) the jump of the specific heat at T_c, $\Delta C_p/(\gamma_n T_c) \approx 2.28$, is well above the value expected for an s-wave BCS SC with $\Delta C_p/(\gamma T_c) \approx 1.43$. This hints at strong-coupling SC. (ii) The temperature-dependent heat capacity below T_c significantly deviates from the universal BCS dependence as indicated by the solid line. Rather, a power law with $C_p(T<T_c) \propto T^3$ is obvious from the experimental data above 3 K (compare Fig. 3), which is sketched by the dashed line as well. Below 3 K, the heat-capacity data reveal an anomaly at about 1 K [see also Fig. 4(a)], which may be attributed either to a tiny fraction of impurity states or to a quite complicated gap structure, where a small fraction of the Fermi surface exhibits a very small gap which opens just at the lowest temperatures. Due to the low-temperature anomaly in the heat capacity it remains unclear whether or not C_{eS} of Mo_3Al_2C is compatible with a nodal structure. A clean exponential temperature dependence is not observed in the present study.

The $1/T_1$ ^{27}Al NMR relaxation rate, taken at $\mu_0 H=1.24$ T and partially at 6.95 T is plotted in Fig. 3(b) on a double logarithmic scale. A Hebbel-Slichter peak right at T_c is absent. This is compatible with a partial disappearance of the SC gap at the Fermi energy, in line with non-s-wave SC. Below T_c, a nonexponential but rather a T^n temperature dependence hints toward a nodal structure, closing partially the SC gap at the Fermi surface. We note that a $1/T_1 \propto T$ component, expected as a signature of a finite impurity density of

states, is clearly absent in our low-temperature data. Volovik and Gork'ov[20] have shown that a proportionality of the density of states according to $N(E) \propto E^m$ results in a NMR relaxation rate $1/T_1 \propto T^{2m+1}$. Thus, an anisotropic gap with nodal structures yields, in general, a T^n power law of $1/T_1$ with $n=3$ for line nodes and $n=5$ for point nodes. Intersecting nodes, however, might modify such simple temperature dependencies.[21] Furthermore, Hayashi *et al.*[22] demonstrated that NCS SCs with mixed spin-singlet and spin-triplet states infer a rather unconventional $1/T_1$ relaxation rate.

Summarized in Fig. 4(a) is the field- and temperature-dependent heat capacity of Mo_3Al_2C, highlighting the suppression of SC upon the application of a magnetic field. The fact that even fields of 11 T do not suppress superconductivity evidences a large upper critical field $\mu_0 H_{c2}$ as well as a large initial slope $\mu_0 H'_{c2}$. The extension of the normal-state behavior toward lower temperatures with rising magnetic fields allows to obtain in a standard manner the Sommerfeld value $\gamma = 17.8$ mJ/mol K^2 and $\theta_D \approx 315$ K [compare Fig. 4(a), inset]. The accurate determination of γ and of $T_c(\mu_0 H)$ was accomplished by idealizing the heat-capacity anomaly under the constraint of entropy balance between the superconducting and the normal state. $T_c(\mu_0 H)$ obtained from Fig. 4(a) is plotted in Fig. 4(b) revealing the upper critical field $\mu_0 H_{c2} > 11$ T and the slope of the upper critical field $\mu_0 H'_{c2} = -3$ T/K.

The temperature dependency of $\mu_0 H_{c2}$ is described following the model of Werthammer *et al.*,[23] incorporating orbital pair breaking, the effect of Pauli spin paramagnetism and spin-orbit scattering. Two parameters, the Maki parameter α (Pauli paramagnetic limitation) (Ref. 24) and spin-orbit scattering λ_{so} specify this model. While an increase in α decrements the upper critical field, an increase in λ_{so} compensates the former, restoring for $\lambda_{so} \to \infty$ a maximum field constrained from orbital pair breaking only. In a first approximation, the Maki parameter α can be derived from γ and ρ_0,[23] resulting in $\alpha = 1.32$. Alternatively, α can be estimated from $\mu_0 H'_{c2}$,[24] revealing $\alpha^* = 1.6$. The sizable Maki parameter of both approximations is an indication that Pauli limiting is non-negligible in Mo_3Al_2C.

TABLE I. Normal-state and SC properties of Mo_3Al_2C.

Crystal structure	Cubic, β-Mn type
Space group	$P4_132$
Lattice parameter	$a = 0.68630$ nm
Sommerfeld value	$\gamma_n = 17.8$ mJ/mol K^2
Debye temperature	$\theta_D = 315$ K
Transport mean-free path	$\lambda_{tr} = 3.06$ nm
Transition temperature	$T_c = 9.0$ K
Electron-phonon enhancement factor	$1 + \lambda_{e,ph} = 1.8$
Upper critical field	$\mu_0 H_{c2}(0) \approx 15.7$ T
Slope of upper critical field	$\mu_0 H'_{c2} = -3$ T/K
Thermodynamic critical field	$\mu_0 H_c(0) = 0.146$ T
Correlation length	$\xi \simeq 4.6$ nm
Ginzburg-Landau parameter	$\kappa_{GL} \simeq 76$
London penetration depth	$\lambda \simeq 380$ nm

Using $\alpha = 1.32$ ($\alpha^* = 1.6$) and $\mu_0 H'_{c2} = -3$ T/K yields $\mu_0 H_{c2}(T)$ as displayed as solid and dashed lines in Fig. 4(b) for $\lambda_{so} = 1.4$ and $\lambda_{so} = 2.5$, respectively, with $\mu_0 H_{c2}(0) \approx 15.7$ T. The Pauli-limiting field follows from $\mu_0 H_p(0) = \sqrt{2}\mu_0 H^*(0)/\alpha$, where $\mu_0 H^*(0) = 18.72$ T, is the Werthamer, Hefland, and Hohenberg (WHH) result for $\alpha = 0$, i.e., the orbital limit. Thus, $\mu_0 H_p(0) = 20$ T for the former and 16.5 T for the latter value of α. These values are in line with $\mu_0 H_p(1.2\ \text{K}) = 15.6$ T reported by Fink *et al.*[25] In the case of strong-coupling superconductivity, these values are further enhanced according to $H_p^{str}(0) = H_p(0)(1+\lambda_{e,ph})^{\epsilon}$ with $\epsilon = 0.5$

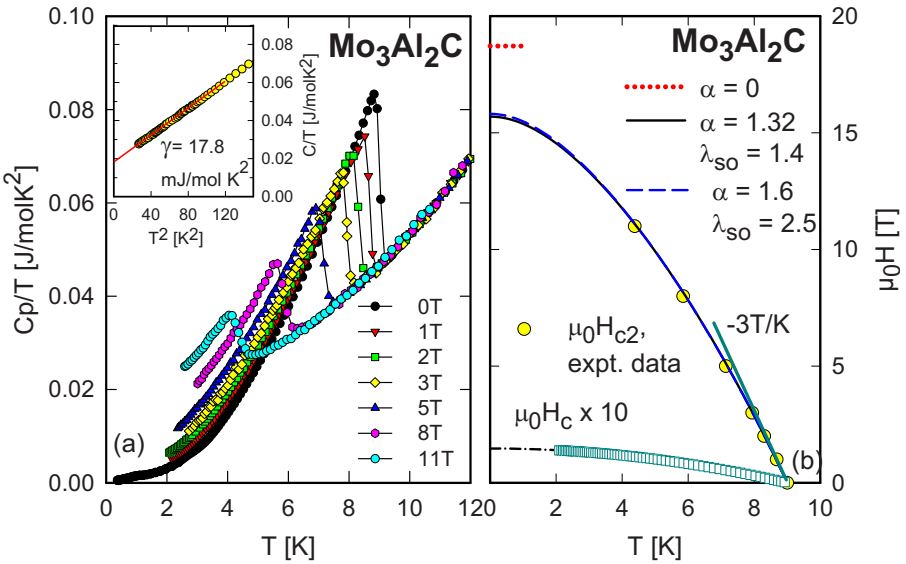

FIG. 4. (Color online) (a) Temperature- and field-dependent specific heat C_p of Mo_3Al_2C. (b) Temperature-dependent upper critical field $\mu_0 H_{c2}$ and thermodynamic critical field $\mu_0 H_c$ as obtained from specific-heat measurements. The solid and the long-dashed lines are fits according to the WHH model for different values of the Maki parameter. The horizontal bar indicates the upper critical field $\mu_0 H^*(0)$ in absence of Pauli limiting. The dashed-dotted line is an extrapolation of the thermodynamic critical field toward zero.

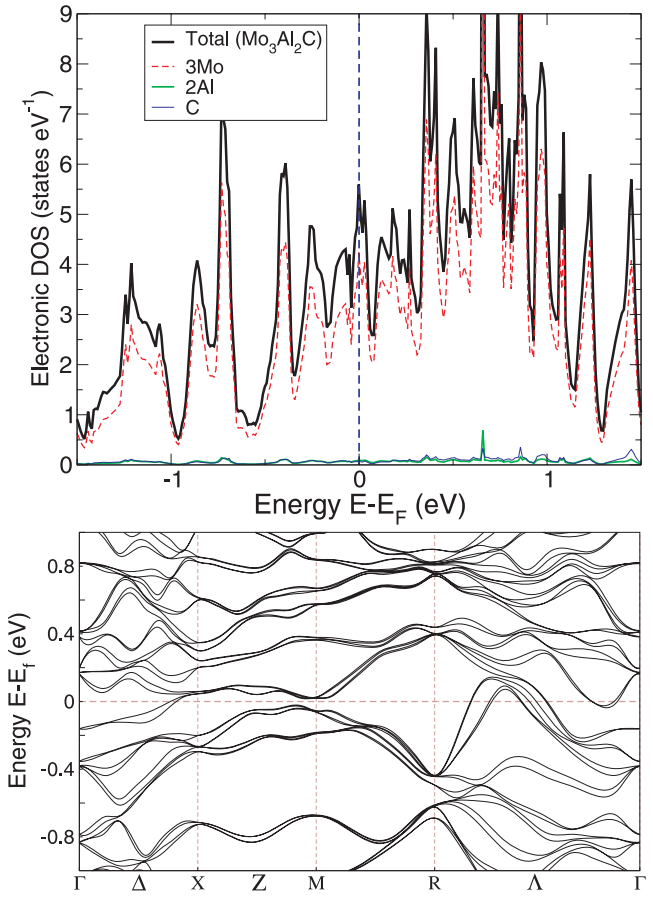

FIG. 5. (Color online) (Upper panel) Section of relativistic total and atom-projected DOS in states per electron volt for Mo_3Al_2C summed over all three Mo atoms for the energy range ± 1.5 eV around the Fermi energy E_F. (Lower panel) Relativistic electronic band structure along high symmetry directions for Mo_3Al_2C in the energy range ± 1 eV around the Fermi energy E_F.

or 1.0.[26,27] Hence, Pauli limiting is not the principal mechanism restricting the upper critical field in Mo_3Al_2C but is present in a relevant size.

The thermodynamic critical field $\mu_0 H_c(T)$ derived in a standard manner from heat-capacity data (compare, e.g., Ref. 8) is shown in Fig. 4(b) by open squares; an extrapolation to $T \to 0$ (dashed-dotted line) yields $\mu_0 H_c(0) \approx 0.146$ T.

SC and normal-state parameters of Mo_3Al_2C can be assessed from γ, $\mu_0 H'_{c2}$, $\mu_0 H_{c2}(0)$, and ρ_0.[26,28] From the Ginzburg-Landau theory with the thermodynamic critical field as primary input, the coherence length, the Ginzburg-Landau parameter and the London penetration depth are calculated. Parameters are summarized in Table I. Based on the estimate $l_{tr}/\xi \approx 0.66$ we classify Mo_3Al_2C as a superconductor in the dirty limit; $\kappa_{GL} \approx 76$ refers to a type-II superconductor.

A section of the calculated electronic DOS of Mo_3Al_2C is shown in Fig. 5 for a relativistic calculation including spin-orbit coupling (upper panel). The DOS around the Fermi energy stems primarily from Mo $4d$ states while the contribution of Al and C is almost negligible. The low partial Al DOS calculated at E_F corresponds well to the NMR Korringa constant, $T_1 T = 11$ sK $[1/T_1 T \propto N(E_F)^2]$. A comparison with Al metal ($T_1 T = 1.8$ sK) reveals a local Al DOS in Mo_3Al_2C of about 3% with respect to the total DFT DOS.

The Fermi energy E_F of Mo_3Al_2C is located in a local maximum of the DOS; its large value favors SC. Employing the Sommerfeld expansion, $N(E_F) = 5.48$ states/eV corresponds to $\gamma_b = 12.9$ mJ/mol K^2, in fair agreement with the experimental Sommerfeld coefficient $\gamma = \gamma_b(1+\lambda_{e,ph}) = 17.8$ mJ/mol K^2.

The lower panel of Fig. 5 displays the DFT electronic band structures along high symmetry directions for Mo_3Al_2C in an energy range ± 1 eV around the Fermi energy. With respect to a nonrelativistic calculation (not shown here), the degenerate bands become split due to the lack of inversion symmetry in Mo_3Al_2C. Specifically, for all bands crossing the Fermi energy the degeneracy is lifted, separating spin-up and spin-down electrons. This provides conditions for the occurrence of spin-singlet and spin-triplet Cooper pairs, leading to two gap functions, where each gap is defined on one of the two bands formed by degeneracy lifting. Superposition of these gaps is presumed to constitute a nodal structure of the resulting SC gap as corroborated from the present experimental data.

In conclusion, electrical resistivity, specific-heat, and NMR measurements classify noncentrosymmetric Mo_3Al_2C as a strong-coupled SC with $T_c = 9$ K. The temperature-dependent specific heat and the $1/T_1$ ^{27}Al NMR relaxation rate deviate from BCS predictions, possibly referring to a nodal structure of the superconducting gap even though SC of Mo_3Al_2C occurs in the dirty limit. Unconventional pairing would be in line with the splitting of electronic bands due to the asymmetric spin-orbit coupling as revealed from relativistic DFT calculations. These split bands might be the cause of a mixing of spin-singlet and spin-triplet Cooper pairs, which otherwise are distinguished by parity,[2] making a nodal structure likely.[22,29] While this proposition has been corroborated for SCs with strong correlations among electrons, specific-heat data unambiguously disprove a strongly correlated electronic state in Mo_3Al_2C. In spite of a lack of correlations, unconventional SC seems to arise from a substantial band splitting and the fact that inversion symmetry is missing in *all* crystallographic directions. In these respects, Mo_3Al_2C is the only example besides isomorphous Li_2Pt_3B.[9]

Note added. Recently, we learned that SC in Mo_3Al_2C was also studied by Karki *et al.*[30] who claimed an exponential temperature dependence of the low-temperature electronic specific heat $C_{eS}(T)$ and concluded that the gap fully opens. We note that the accuracy of low-temperature electronic specific-heat data obtained by subtracting a phonon contribution extremely depends on the accuracy by which the normal-state heat capacity has been determined from high-field measurements. The low-temperature electronic heat capacity $C_{eS}(T < 2.5$ K) obtained in the present study clearly deviates from that proposed in Ref. 30 [see dashed-dotted line in Fig. 3(a)].

Work supported by the Austrian Science Foundation FWF under Grant No. P22295. X.-Q.C. acknowledges the support from the "Hundred Talents Project" of CAS.

[1] L. E. Toth and J. Zbasnik, Acta Metall. **16**, 1177 (1968).
[2] L. P. Gor'kov and E. I. Rashba, Phys. Rev. Lett. **87**, 037004 (2001).
[3] E. Bauer, G. Hilscher, H. Michor, C. Paul, E. W. Scheidt, A. Gribanov, Yu. Seropegin, H. Noël, M. Sigrist, and P. Rogl, Phys. Rev. Lett. **92**, 027003 (2004).
[4] T. Akazawa, H. Hidaka, T. Fujiwara, T. C. Kobayashi, E. Yamamoto, Y. Haga, R. Settai, and Y. Onuki, J. Phys.: Condens. Matter **16**, L29 (2004).
[5] N. Kimura, K. Ito, K. Saitoh, Y. Umeda, H. Aoki, and T. Terashima, Phys. Rev. Lett. **95**, 247004 (2005).
[6] I. Sugitani Y. Okuda, H Shishido, T. Yamada, A. Thamizhavel, E. Yamamoto, T. D. Matsuda, Y. Haga, T. Takeuchi, R. Settai, and Y. Onuki, J. Phys. Soc. Jpn. **75**, 043703 (2006).
[7] T. Takimoto and P. Thalmeier, J. Phys. Soc. Jpn. **78**, 103703 (2009).
[8] E. Bauer, R. T. Khan, H. Michor, E. Royanian, A. Grytsiv, N. Melnychenko-Koblyuk, P. Rogl, D. Reith, R. Podloucky, E.-W. Scheidt, W. Wolf, and M. Marsman, Phys. Rev. B **80**, 064504 (2009).
[9] H. Q. Yuan, D. F. Agterberg, N. Hayashi, P. Badica, D. Vandervelde, K. Togano, M. Sigrist, and M. B. Salamon, Phys. Rev. Lett. **97**, 017006 (2006).
[10] L. E. Toth, in *Transition Metal Carbides and Nitrides*, Refractory Materials Monographs Vol. 7, edited by J. L. Margrave (Academic Press, New York, 1971).
[11] J. Rodríguez-Carvajal, Physica B **192**, 55 (1993).
[12] E. Bauer, St. Berger, Ch. Paul, M. D. Mea, G. Hilscher, H. Michor, M. Reissner, W. Steiner, A. Grytsiv, P. Rogl, and E. W. Scheidt, Phys. Rev. B **66**, 214421 (2002).
[13] E. Bauer, H. Kaldarar, R. Lackner, H. Michor, W. Steiner, E.-W. Scheidt, A. Galatanu, F. Marabelli, T. Wazumi, K. Kumagai, and M. Feuerbacher, Phys. Rev. B **76**, 014528 (2007).
[14] G. Kresse and J. Furthmüller, Phys. Rev. B **54**, 11169 (1996); G. Kresse and D. Joubert, *ibid.* **59**, 1758 (1999).
[15] J. Johnston, L. Toth, K. Kennedy, and E. R. Parker, Solid State Commun. **2**, 123 (1964).
[16] O. Gunnarsson, M. Calandra, and J. E. Han, Rev. Mod. Phys. **75**, 1085 (2003).
[17] W. L. McMillan, Phys. Rev. **167**, 331 (1968).
[18] N. N. Bogoliubov, V. V. Tolmachov, and D. V. Shirkov, Fortschr. Phys. **6**, 605 (1958).
[19] B. Mühlschlegel, Z. Phys. **155**, 313 (1959).
[20] G. E. Volovik and L. P. Gork'ov, Sov. Phys. JETP **61**, 843 (1985).
[21] Y. Hasegawa, J. Phys. Soc. Jpn. **65**, 3131 (1996).
[22] N. Hayashi, K. Wakabayashi, P. A. Frigeri, and M. Sigrist, Phys. Rev. B **73**, 092508 (2006).
[23] N. R. Werthamer, E. Hefland, and P. C. Hohenberg, Phys. Rev. **147**, 295 (1966).
[24] K. Maki, Phys. Rev. **148**, 362 (1966).
[25] H. J. Fink, A. C. Thorsen, E. Parker, V. F. Zackay, and L. Toth, Phys. Rev. **138**, A1170 (1965).
[26] T. P. Orlando, E. J. McNiff, Jr., S. Foner, and M. R. Beasley, Phys. Rev. B **19**, 4545 (1979).
[27] M. Schossmann and J. P. Carbotte, Phys. Rev. B **39**, 4210 (1989).
[28] See, for example, M. Tinkham, *Introduction to Superconductivity* (McGraw-Hill, New York, 1975).
[29] P. A. Frigeri, D. F. Agterberg, A. Koga, and M. Sigrist, Phys. Rev. Lett. **92**, 097001 (2004).
[30] A. B. Karki, Y. M. Xiong, I. Vekhter, D. Browne, P. W. Adams, D. P. Young, K. R. Thomas, J. Y. Chan, H. Kim, and R. Prozorov, Phys. Rev. B **82**, 064512 (2010).